

# Influence of Microstrip Probe Pad Design on Planar Measurements Using On-Wafer Probes

Patrick Seiler, Bernhard Klein, Dirk Plettemeier  
Chair for RF and Photonics Engineering, Communications Laboratory  
Faculty of Electrical and Computer Engineering  
Technische Universität Dresden, Germany  
Email: patrick.seiler@tu-dresden.de

**Abstract**—This publication refers to work previously published by the authors at ISAP 2014. There, it has been shown how measurements with an on-wafer probe on planar transmission lines up to 67 GHz can be used for the determination of the transmission line’s substrate permittivity. Especially the microstrip probe pad on the substrate, which represents the probe-microstrip interface, has shown to be of significant influence on the measurement data, which allowed measurements up to only 25 GHz. The work presented in this paper gives measurement data with a doubled frequency limit of 50 GHz. Additionally, different sources of interference such as coupling, higher modes and probe pad design are discussed. An example for a broadband transition from on-wafer probe to microstrip is shown, which can be used for on-wafer or PCB antenna measurements up to 200 GHz. Finally, design rules on how to avoid the deteriorating effect on measurement data are given.

## I. INTRODUCTION

Today’s demand for antennas for applications in the microwave regime, such as imaging at about 94 GHz [1] or even chip-to-chip communication at about 180 GHz [2], requires antennas to be fabricated in planar technology. Especially with increasing frequency, on-chip antennas or antennas fabricated on a PCB substrate specifically designed for RF applications often become the only way of realizing appropriate antennas for the desired application. For measurement and characterization, on-wafer probes are commonly used to contact such antennas [3], [4].

To test such a planar antenna using on-wafer probes prior to complete integration of the antenna in a package or chip, it is usually placed separately on the substrate, only with a short transmission line (TL) contacting a pad structure. This pad structure serves as probe-TL interface for the actual on-wafer probe. The probe is then used to contact the pad structure and therefore antenna to be tested. Before that, a calibration is applied, so that the disturbance by the pad structure or additionally the transmission line contacting the antenna can be neglected or even de-embedded from the actual antenna measurement.

In work previously published by the authors at ISAP 2014 [5], such pad structures were used for measurements of transmission lines up to 67 GHz. Prior to that, a thru-reflect-line (TRL) calibration has been applied, which is considered a rather robust calibration technique and even allows for a complete de-embedding of the interfacing structure. Never-

theless, comparing the measured transmission lines<sup>1</sup>, only the microstrip (MS) has shown extensive data corruption, resulting in measurements being made up to only 25 GHz instead of 67 GHz. As will be shown in this paper, the general design of the pad structure itself has a strong influence on the frequency behaviour of the overall measurement. This influence could not be corrected by the applied calibration and de-embedding technique.

Therefore, in this paper several potential influence factors for the observed deviation are investigated. Subsequently, an optimized microstrip probe pad structure will be presented, which allows measurements up to 200 GHz.

## II. MEASUREMENT AND RESULTS

For all measurements, a set of GGB Picoprobes™ Model 67A in ground-signal-ground (GSG) configuration with a pitch of 400  $\mu\text{m}$  and a Network Analyzer up to 67 GHz on a wafer probing station have been used. The MS measured have been fabricated on a Rogers Corp. Ultralam™ 3850 PCB substrate [6], see Tab. I for relevant dimensions<sup>2</sup>.

TABLE I  
MEASURED MS ON ULTRALAM™3850 ( $\epsilon_r = 3.05$ ).

substrate height	100 $\mu\text{m}$
strip width	240 $\mu\text{m}$
strip-to-ground gap	200 $\mu\text{m}$

A picture of the actual MS probe pad structure is given in Fig. 1, left. It consists of vias from top to bottom ground and a launch for the actual microstrip.

The copper surface of the MS has been gold-plated to avoid deterioration through oxidation.

The layout is given in Fig. 2 and consists of four transmission lines with a length of 2.5 cm for the actual measurement in the upper section, as well as multiple sets of custom TRL calibration standards in the lower section.

These calibration standards have been used to perform a multiline TRL calibration [7] prior to the measurements.

<sup>1</sup>The aforementioned publication has shown measurements on microstrip, coplanar waveguide and grounded coplanar waveguide.

<sup>2</sup>Here, “strip-to-ground gap” refers to the distance from the actual microstrip launch to the edge of the upper ground metallization.

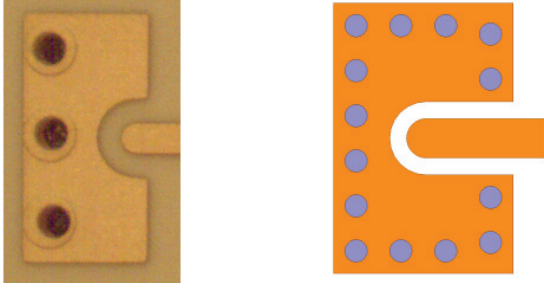


Fig. 1. Actual MS probe pad structure including vias (left), new pad structure used for simulations as discussed in Sec. III (right).

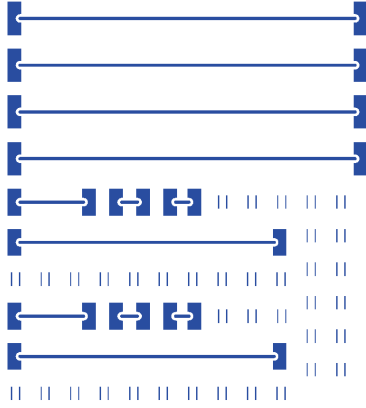


Fig. 2. Layout consisting of MS transmission lines for measurement (top) and a set of custom TRL calibration standards (bottom).

For the sake of a simple representation without neglecting any of the four measured S-Parameters, the authors decided to combine them into the transmission coefficient (T) and reflection coefficient ( $\Gamma$ ), whose connection to the S-Parameters can be seen using signal flow graph theory [8]:

$$S_{11} = S_{22} = \frac{(1 - T^2)\Gamma}{1 - \Gamma^2 T^2} \quad (1)$$

$$S_{21} = S_{12} = \frac{(1 - \Gamma^2)T}{1 - \Gamma^2 T^2} \quad (2)$$

Combining (1) and (2), the coefficients can be expressed by the S-Parameters:

$$T = \frac{(S_{11} + S_{21}) - \Gamma}{1 - (S_{11} + S_{21})\Gamma} \quad (3)$$

$$\Gamma = K \pm \sqrt{K^2 - 1} \quad (4)$$

$$K = \frac{S_{11}^2 - S_{21}^2 + 1}{2S_{11}}, \quad (5)$$

where the sign in (4) is chosen so that  $|\Gamma| \leq 1$ , which is required for causal, passive materials.

The results for T and  $\Gamma$  for the measured MS are given in Fig. 3, top. As can be seen, the data is consistent up to about 50 GHz.

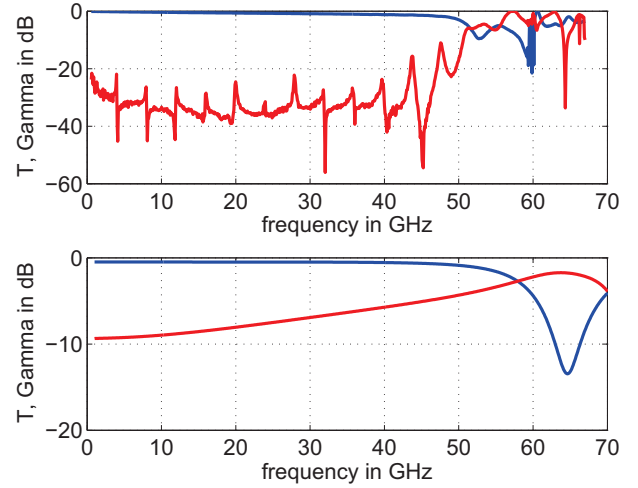


Fig. 3. T (blue) and  $\Gamma$  (red) for measurement of MS (top) and simulation of probe pad (bottom).

For higher frequencies, the measurement data becomes inconsistent and shows a resonant behaviour.

The data given for MS measurements in the author's previous publications extended only up to 25 GHz, see [5] and [9] for reference. The MS transmission lines there were fabricated on a Rogers Corp. RO4003C<sup>TM</sup> PCB substrate with a height of 203  $\mu\text{m}$  and slightly different planar dimensions. Originally, the authors assumed that the deviations above 25 GHz would be due to fabrication issues of the probe-MS interface structure on the substrate, since there was a slight overetching present. Due to this overetching, the ground tip of the GSG-style probe was very near the edges of the ground plane, so that for higher frequencies improper contacting was assumed to be the source of the deviations, which resulted in the corrupted measurement data. To avoid this placement problem and undesired frequency response, the PCB layout presented in this paper has been designed and fabricated, to assure sufficient space for all probe tips to be placed properly on the metallized surface.

### III. DISCUSSION OF INFLUENCE FACTORS ON THE UPPER FREQUENCY LIMIT

However, on the new measurement data, the same influence and data corruption can be seen for frequencies higher than about 50 GHz, see Fig. 3, top. Coupling of adjacent microstrip lines on the layout, the excitation of higher modes of the MS and the probe pad structure will be discussed as influence factors in the following. All simulations mentioned have been made using ANSYS<sup>TM</sup> Electromagnetics Suite, if not mentioned otherwise.

#### A. Coupling of adjacent microstrip lines

Since there are several microstrip lines in close proximity to each other on the layout (see Fig. 2), coupling could be a possible reason for the observed resonant behaviour.

However, simulations of two single, adjacent microstrip lines show, that the crosstalk is lower than -20 dB for every frequency up to 67 GHz. Therefore, this effect should be neglectable as a potential influence factor.

During the calibration measurements, there are several calibration standards such as microstrip lines of different length or shortening bars in close proximity to each other. The simulation of all these structures is rather complex. Additionally, the results for two adjacent microstrips give no measure for a potential influence due to coupling during calibration. Therefore, the authors decided to investigate this by measurement instead. To assure that there is no deteriorating influence due to coupling effects during calibration, a full set of calibration standards as well as a MS for measurement after calibration have been separated and glued in arbitrary locations and distance to a block of teflon, see Fig. 4.

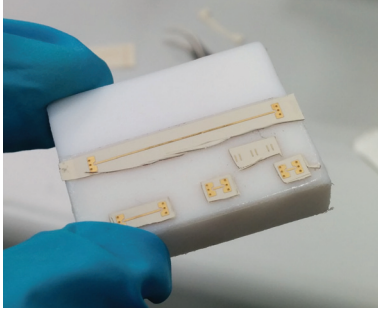


Fig. 4. Separated MS transmission line as well as a set of custom TRL calibration standards glued to a block of teflon.

The data obtained by calibrating using the separated calibration standards and measurement of the separated MS afterwards is about identical to the data given in Fig. 3, blue. Therefore, the overall effects of coupling are considered to be neglectable.

### B. Higher modes in MS transmission lines

Higher modes in transmission lines often show a resonant behaviour due to the reoccurring coupling frequencies to the fundamental mode of the microstrip [10] and thus could be an explanation for the observed behaviour. As given in [10] and explained by the authors in [9], two kinds of higher modes in MS exist. The cutoff frequencies of these modes are given by:

$$f_{r, TM_0} = \frac{c_0 \arctan(\epsilon_r)}{\pi h \sqrt{2(\epsilon_r - 1)}}, \quad (6)$$

where  $c_0$  stands for the velocity of light in vacuum,  $\epsilon_r$  for the substrate permittivity and  $h$  for the substrate height, and

$$f_{c, MS} = \frac{c_0}{2w_{\text{eff}} \sqrt{\epsilon_{r, \text{eff}}}}, \quad (7)$$

where  $w_{\text{eff}}$  stands for the effective strip width of the MS conductor, see [11].

Using the values as given in Tab. I, both cutoff frequencies  $f_{r, TM_0} = 591$  GHz and  $f_{c, MS} = 383$  GHz are higher than the measurement range of 67 GHz. Therefore, the influence due to higher modes can be neglected as well.

### C. Influence of MS probe pad structure

The MS probe pad structure used, however, shows a significant influence on the actual S-Parameters of the MS. The pad structure of the measured MS has been simulated, T and  $\Gamma$  obtained from simulated S-Parameters can be seen in Fig. 3, bottom.

The MS has been modelled only as the probe pad structure and a short section of the actual microstrip line to decrease simulation time by keeping the simulation model small. Therefore, no resonances due to transmission line length occur within the reflection coefficient. Additionally, the measured data has been calibrated prior to measurements, which gives an explanation for the overall smaller attenuation (higher transmission) and reflection coefficient in the measurement data.

However, the general effect on the parameters is recognizable in both plots for simulation as well as measurement, and even the frequency response and peak above 50 GHz is comparable: The decrease of transmission and increase of reflection have a very similar shape in the range from 50 GHz to 60 GHz. At about 60 GHz, the corrupted measurement data looks rather unphysical, which suggests problems with the calibration<sup>3</sup>. Since this deterioration of measurement data quality is not related to coupling during calibration as shown above, the authors consider it a reasonable conclusion, that mainly the probe pad structure has an influence on the measurement. The magnitude of this influence is high enough, so that the applied TRL calibration could not correct this effect.

Since the simulation data suggests some kind of resonance of the overall structure, it is necessary to push any resonances within the frequency range being measured to higher frequencies to suppress the undesired behaviour. A further simulation on a significantly smaller probe pad structure (see Tab. II for dimensions and Fig. 1, right for schematic) with increased number of vias has been done, where Polyamide with a height of 30  $\mu\text{m}$  has been used as substrate material during simulation<sup>4</sup>.

TABLE II  
SIMULATED MS ON POLYAMIDE ( $\epsilon_r = 2.9$ ).

substrate height	30 $\mu\text{m}$
strip width	70 $\mu\text{m}$
strip-to-ground gap	30 $\mu\text{m}$

Here, T and  $\Gamma$  show reasonable behaviour, so that the MS transmission line using this pad structure can be measured over the whole frequency range from DC up to 200 GHz for further measurements.

Fig. 5, top gives data for this new pad structure and Fig. 5, bottom shows an extended simulation of the probe pad

<sup>3</sup>Based on the authors' measurement experience.

<sup>4</sup>The authors decided to use these structure sizes and material, since they plan to realize the new probe pad structure on a commercially available process [12] in the near future. Instead, any available back end of line or thin film process with equivalent choice of structure dimensions and material platform can be used for the fabrication as well.

structure as mentioned before for comparison.

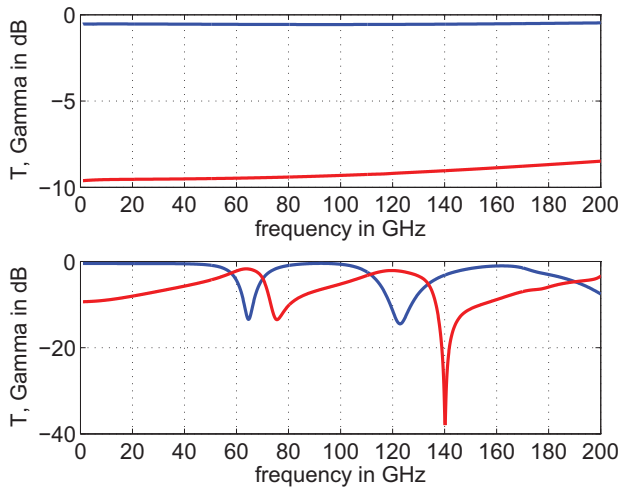


Fig. 5. Simulation data for new probe pad structure (top) and the probe pad structure used for measurements (bottom).

As can be seen, the original pad structure shows significant resonant behaviour, whereas this effect can be suppressed totally by using the new structure. The authors explain this as follows:

The current is originally fed to the pad structure by the on-wafer probe contacting it from above. Then, it takes an arbitrary path to the ground on the bottom of the substrate through the metallized ground plane on the top and the vias. This current path can be seen as a RLC circuit, whose resonant frequency is proportional to  $\omega = \frac{1}{\sqrt{LC}}$ , where L and C denote the inductance and capacitance, respectively. Each path can be interpreted as a single discontinuity adding to the inductive behaviour, since the current lags behind the voltage due to the difference in path length: The path length for the current is given by the distance from probe tip to via along the top metallization and the via height. The effective path for the voltage can be seen as the fundamental mode of the electrical field and thus a direct field line or path from the MS center conductor to the bottom ground. These path differences result in a phase shift between current and voltage and hence the reactive behaviour.

To avoid this behaviour, the effective current path has to be decreased. This has been done for the new probe pad, since the via height and distances from the probe tips to the vias have been reduced significantly, resulting in a reduced overall inductivity. Additionally, with an increased number of vias, the new pad structure consists of more inductive discontinuities connected in parallel, resulting in a reduced overall inductivity of the structure. Therefore, both aforementioned design choices decrease the overall inductivity of the new probe pad ( $L \downarrow$ ) and thus the resonances can be moved to higher frequencies ( $\omega \uparrow$ ). During our simulations it appeared, that the foremost vias (seen in propagation direction of the wave along the MS) have a slightly bigger influence on the increase

in frequency than the vias in the back of the probe pad. Since these vias offer the shortest path to the bottom ground as they force the current to flow in the wave's propagation direction, the phase shift between current and voltage is the smallest compared to other paths. This observation is consistent with the explanation just presented.

#### IV. CONCLUSION

Different influence factors on the MS probe pad structure such as coupling between adjacent microstrips, higher modes and the actual layout of the probe pad structure have been discussed. The main influence by the probe pad structure has been explained physically. As a general rule for MS probe pad design, the effective current path and therefore lag behind the voltage should be kept to a minimum, which can be achieved by decreasing the substrate height and distances from the probe tips to the vias. Microstrip measurements up to 24 GHz previously presented by the authors could be increased to 50 GHz and a MS probe pad structure has been shown, which can be used for measurements up to 200 GHz.

#### ACKNOWLEDGMENT

This work is supported by the German Research Foundation (DFG) in the Collaborative Research Center 921 "Highly Adaptive Energy-Efficient Computing".

#### REFERENCES

- [1] M. Seyyed-Esfahlan, I. Tekin, and M. Kaynak, "Wideband 94 GHz on-chip dipole antennas for imaging applications," in *Antennas and Propagation Society International Symposium*, 2014.
- [2] B. Klein, M. Jennings, P. Seiler, and D. Plettemeier, "Wideband half-cloverleaf shaped on-chip antenna for 160 GHz - 200 GHz applications," in *Antennas and Propagation Society International Symposium*, 2014.
- [3] Z.-M. Tsai, Y.-C. Wu, S.-Y. Chen, T. Lee, and H. Wang, "A v-band on-wafer near-field antenna measurement system using an ic probe station," *Antennas and Propagation, IEEE Transactions on*, 2013.
- [4] B. Klein, M. Jennings, P. Seiler, K. Wolf, and D. Plettemeier, "Verification and demonstration up to 67 GHz of an on-chip antenna pattern measurement setup," in *IEEE Conference on Antenna Measurements & Applications*, 2014.
- [5] P. Seiler, B. Klein, and D. Plettemeier, "Broadband characterization of planar transmission line substrate permittivity up to 67 GHz," in *International Symposium on Antennas and Propagation*, 2014.
- [6] *Data sheet: Ultralam<sup>®</sup> 3000 - Liquid Crystalline Polymer Circuit Material*, Rogers Corporation. [Online]. Available: <http://www.rogerscorp.com/documents/730/acs/ULTRALAM-3000-LCP-laminate-data-sheet-ULTRALAM-3850.pdf>
- [7] R. B. Marks, "A multilayer method of network analyzer calibration," *Microwave Theory and Techniques, IEEE Transactions on*, vol. 39, no. 7, pp. 1205-1215, Jul 1991.
- [8] A. Nicolson and G. F. Ross, "Measurement of the intrinsic properties of materials by time-domain techniques," *Instrumentation and Measurement, IEEE Transactions on*, vol. 19, no. 4, pp. 377-382, Nov 1970.
- [9] P. Seiler, B. Klein, and D. Plettemeier, "Analytical and experimental investigation of substrate permittivity and loss up to 67 GHz," in *Asia-Pacific Conference on Communications*, 2014.
- [10] R. K. Hoffmann, *Handbook of Microwave Integrated Circuits*. Artech House Microwave Library, 1987.
- [11] K. C. Gupta, *Microstrip Lines and Slotlines 2nd Ed.* Artech House Microwave Library, 1996.
- [12] *Thin Film Multilayer Process*, Hightec MC AG. [Online]. Available: <http://hightec.ch/technology/thin-film-process/>